Electrochimica Acta 317 (2019) 766–777

Contents lists available at ScienceDirect

Electrochimica Acta

journal homepage: www.elsevier.com/locate/electacta

Novel nanocomposite film modified electrode based on poly(brilliant cresyl blue)-deep eutectic solvent/carbon nanotubes and its biosensing applications

Wanderson da Silva, Mariana Emilia Ghica, Christopher M.A. Brett*

Department of Chemistry, Faculty of Sciences and Technology, University of Coimbra, 3004-535 Coimbra, Portugal

ARTICLE INFO

Article history:
Received 3 April 2019
Received in revised form
31 May 2019
Accepted 1 June 2019
Available online 6 June 2019

Keywords:
Deep eutectic solvent
Ethaline
Brilliant cresyl blue
Electropolymerization
Enzyme biosensors

ABSTRACT

Electropolymerization of brilliant cresyl blue (BCB) in ethaline deep eutectic solvent (DES) has been carried out. Poly(brilliant cresyl blue) (PBCB) films were formed by electrodeposition on carbon nanotube modified glassy carbon electrodes by potential cycling in ethaline (choline chloride + ethylene glycol) with the addition of different ionic species i.e. NO_3^-, SO_4^{2-}, Cl^-, ClO_4^-. The novel nanocomposite films were characterized by scanning electron microscopy, cyclic voltammetry and electrochemical impedance spectroscopy. The composition of the polymerization solution had a large influence on the morphology as well as on the electrochemical behaviour of the electrodeposited films. The effect of scan rate on BCB polymerization was also investigated and the PBCB film synthesized at 150 mV s^{-1} in ethaline + NO_3^- presented a superior electrochemical performance. The $PBCB_{Ethaline}$-HNO_3/MWCNT and $PBCB_{aqueous}$/MWCNT nanocomposite films were used as electrode support for the enzymes glucose oxidase and tyrosinase for the biosensing of glucose and catechol, respectively and were more sensitive than the PBCB based electrodes prepared in aqueous solution.

1. Introduction

Conducting polymers have remarkable electronic, optical, electrochromic, electroluminescent, chemosensitive, and conductivity properties, being applicable in different research fields such as solar cells, batteries, electrochemical sensors and biosensors [1–3]. However, when used as substrates for enzyme immobilization in biosensing applications the results are not always so promising due to the low catalytic current obtained [4,5]. This can be overcome by choosing a suitable monomer capable of forming a polymeric conducting film which itself has redox properties and is biocompatible. Azine dye polymer films can address this problem through their ability to act as electron donors/acceptors in enzyme reactions, promoting long-term stability and catalytic efficiency [6,7]. Brilliant cresyl blue (BCB) is a cationic quinine-amine phenazine dye with a planar rigid structure, the corresponding polymer having promising properties as a redox conducting polymer with good electrocatalytic properties, fast rate of charge transfer, and ion transport, and can be synthesized by electrochemical polymerization [4,8]. Recently, PBCB-modified electrodes prepared by polymerization in aqueous solution have been reported [4,6,7,9–11].

Despite the excellent properties mentioned above, polymer dye films electrogenerated in aqueous solution can result in an unstable material, which can detach from the electrode to the solution and compromise sensor response. Ionic liquids (ILs) have been successfully used as solvents for radical polymerization, enhancing polymerization rates and leading to the formation of higher molecular weight and more stable polymers than those formed in aqueous electrolytes. This has been attributed to a reduction in activation energy for polymerization and the formation of a solvation sphere around propagating radicals, creating “protected radicals”, thus increasing the polymerization rate and mass of the material electrodeposited [12,13]. Deep eutectic solvents (DES), have emerged as another alternative medium for polymer synthesis due to the formation of a material with controlled nanostructure [14]. A DES is defined as a binary mixture of at least two components, a hydrogen bond acceptor (HBA) and a hydrogen bond donor (HBD) with a composition corresponding to the eutectic point [15]. DES have properties in common with ILs, such as a large working temperature range, good chemical stability and wide

* Corresponding author.
E-mail address: cbrett@ci.uc.pt (C.M.A. Brett).

https://doi.org/10.1016/j.electacta.2019.06.003
0013-4686/

electrochemical window that is important for polymer electrosynthesis, which often requires a high potential for radical generation. Additionally, compared to ILs, DES have easier preparation at lower cost, do not require exhausting steps of preparation and/or purification and are normally biodegradable [16–18].

The combination of multiwalled carbon nanotubes (MWCNT) with polymers is beneficial for sensor applications, since this combination normally leads to an improved performance sensing device, because of their complementary electrical and catalytic properties [19], as well as a significant increase in active surface area upon electrode modification by MWCNT.

The present work focuses on the development and characterization of a novel electrode architecture based on the redox polymer PBCB electrodeposited in ethaline DES on a MWCNT-modified glassy carbon electrode and its evaluation for biosensing applications. In order to increase the ionic strength of the solution of BCB in ethaline during BCB polymerization, the influence of adding small quantities of different acids (HNO_3, H_2SO_4, HCl, and $HClO_4$) was tested. The best conditions were chosen for $PBCB_{ethaline}$/MWCNT nanocomposite film fabrication and comparison made with PBCB films formed in aqueous solution. Scanning electron microscopy (SEM) was used to examine the influence of the electrolyte composition on the morphology of the nanocomposite films. Cyclic voltammetry (CV), electrochemical impedance spectroscopy (EIS), and differential pulse voltammetry (DPV) were employed to evaluate the electrochemical behaviour of the nanocomposite films. Finally, the nanocomposite-modified electrode with the best sensing properties was evaluated for biosensing applications using two model enzymes: glucose oxidase and tyrosinase.

2. Experimental

2.1. Reagents and solutions

The reagents were all analytical grade and were used as received. Tyrosinase (Tyr, from mushroom, activity 2687 U mg^{-1}, CAS number: 9002-10-2), glucose oxidase (GOx, from *Aspergillus niger*, type X–S, activity 250 U mg^{-1}, CAS number: 9001-37-0), bovine serum albumin (BSA), 98%, glutaraldehyde (GA)(25% v/v in water), choline chloride, chitosan from crab shells, minimum 85% deacetylated**,** ethylene glycol, nitric acid (65%), sulfuric acid (98%), hydrochloric acid (37%), acetic acid (99.99%), and perchloric acid (70%) were acquired from Sigma-Aldrich, Germany. Brilliant cresyl blue was purchased from Fluka, Switzerland. Multiwalled carbon nanotubes (MWCNT) with ~95% purity, 30 ± 10 nm diameter, and 1–5 μm length were from Nanolab, U.S.A**.** Britton-Robinson (BR) buffer supporting electrolyte was made by mixing phosphoric acid, acetic acid and boric acid (all solutions of 0.040 M concentration) and adjusting the pH with 0.5 M sodium hydroxide and used for polymer film characterizations. The phosphate buffer (PB) solution, pH 7.0, was prepared by mixing NaH_2PO_4 and $Na_2HPO_4 \cdot 2H_2O$ in the appropriate proportion and used as supporting electrolyte for biosensor evaluation. Millipore Milli-Q nanopure water (resistivity ≥ 18 MΩ cm) was used for the preparation of all solutions. All experiments were performed at room temperature (25 ± 1 °C).

2.2. Instrumentation

Voltammetric experiments were performed with an Ivium CompactStat potentiostat (version 2.024, Ivium Technologies, Netherlands) using a conventional three electrodes cell consisting of a glassy carbon electrode (GCE) (geometric area 0.00785 cm^2) or GCE modified as working electrode, a platinum wire as counter electrode and an Ag/AgCl (3 M KCl) electrode was used as reference. Electrochemical impedance measurements were carried out with a Solartron 1250 Frequency Response Analyser coupled to a Solartron 1286 electrochemical interface using ZPlot 2.4 software (Solartron Analytical, UK). A sinusoidal voltage perturbation of amplitude 10 mV rms was applied in the frequency range between 65 kHz and 0.1 Hz with 10 frequency steps per decade. Equivalent circuit fitting was done with ZView 3.2 software (Scribner Associates, USA). A scanning electron microscope (SEM) (JEOL, JSM-5310, Japan) was used to characterize the morphology of the nanostructured nanocomposites on carbon film electrodes. The pH measurements were carried out with a CRISON 2001 micropH-meter (Crison Instruments SA, Barcelona, Spain) at room temperature.

2.3. Functionalization of the multiwalled-carbon nanotubes (MWCNT) and electrode preparation

Because of the hydrophobic nature of the MWCNT and the presence of metallic impurities obtained from the process of synthesis, its functionalization and purification are necessary before use as a modifier. The procedure described in Ref. [20] was followed. First, an appropriate amount of MWCNT in a 5 M nitric acid aqueous solution was stirred for 24 h, in order to create defects, more edge sites and ensure a better dispersion of the carbon nanotubes by the creation of carboxylic groups. The latter refers to the creation of terminal carbons in the shortening of nanotubes, which upon oxidation are converted into carboxyl groups. Afterwards, the functionalized MWCNT were rinsed with Milli-Q water on a Millipore filter paper (0.3 μm) until a neutral pH was reached, then were collected and dried at 80 °C overnight.

In order to ensure a stabilized and adherent MWCNT layer on the electrode surface, a dispersion of MWCNT in chitosan solution was prepared. Chitosan possesses reactive amino and hydroxyl groups, the positive amino group ensures electrostatic interaction with negative carboxyl groups of the carbon nanotubes, leading to a robust structure. Furthermore, chitosan has a high permeation to water and ions, good mechanical strength, high film-forming ability and is an excellent matrix for biomolecule immobilization. It has been used in enzyme biosensors as binding molecule due to the electrostatic interaction between its negative hydroxyl and positive charges of the amino groups in enzymes [21]. A 1.0% w/v MWCNT-chitosan solution was prepared by weighing 1 mg of dried MWCNT followed by dispersion in 100 μL of 1.0% w/v chitosan solution, previously dissolved in 1.0% v/v acetic acid solution. The mixture was then sonicated for 2 h to obtain a homogeneous solution.

Before modification with carbon nanotubes, the bare GCE was polished with diamond spray (Kemet, UK) with 6 μm, 3 μm, and finally 1 μm particle size. Then it was rinsed with Milli-Q water and sonicated to guarantee the removal of adherent solid particles. After the cleaning step, the MWCNT/GCE was prepared by casting 2 μL of the previously prepared dispersion of MWCNT-chitosan on the GCE and drying at room temperature.

2.4. BCB polymerization

Ethaline melt was prepared by mixing choline chloride and ethylene glycol in a 1:2 ratio. The solid choline chloride was preheated at 80 °C to evaporate the excess of water followed by the addition of ethylene glycol. The mixture was then stirred and heated up to 100 °C until a homogenous and colourless solution of ethaline was formed. After cooling down to room temperature, this was used for the preparation of BCB polymerization solutions. In pure ethaline, BCB electropolymerization was not effective, since there is no appearance of polymer current peaks. DES by itself has a low conductivity that can be made higher by increasing the ionic

strength of the solution that also increases the rate of diffusion of species. This can be achieved by the addition of small amounts of different acids to DES. First, a solution of 0.1 mM BCB in 10 mL ethaline was prepared, to which a small volume (less than 100 μL) of different concentrated acids (HNO_3, H_2SO_4, HCl, and $HClO_4$) was added, to obtain a final concentration of 0.5 M of acid. PBCB was potentiodynamically electrodeposited on MWCNT/GCE by cycling during 30 scans in the potential range from −0.6 to +1.0 V at scan rates in the range from 50 to 200 mV s^{-1}. For comparison, PBCB was also prepared in an aqueous solution containing: 0.1 mM BCB +0.1 M KNO_3 + 0.1 M PB (pH 7.0) at a scan rate of 50 mV s^{-1} as optimized in Ref. [4]. Polymerization of BCB in aqueous acidic media only occurred to a very small extent.

2.5. Biosensor preparation

In order to assess the biosensing properties of the MWCNT/GCE modified with $PBCB_{ethaline}$ films, $PBCB_{aqueous}$ films, and bare GCE, two enzymes, glucose oxidase (GOx) and tyrosinase (Tyr) were immobilized for the detection of glucose and catechol, respectively. For enzyme solution preparation, 2.0% w/v of GOx or Tyr was dissolved in 100 μL of 0.1 M PB solution (pH 7.0) containing BSA (2.0%

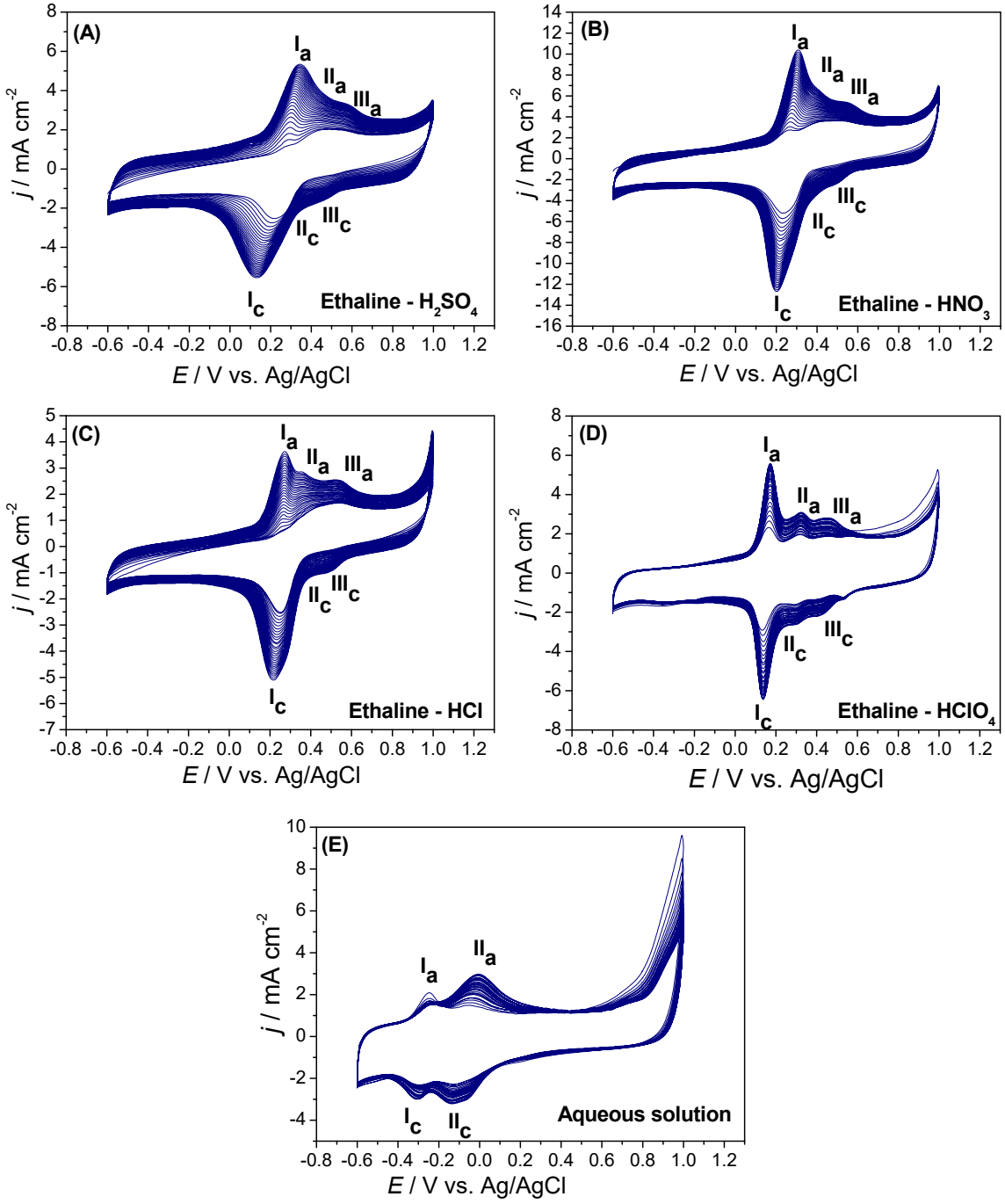

Fig. 1. Potential cycling electrodeposition of PBCB on MWCNT/GCE at scan rate 50 mV s^{-1} from a solution containing 0.1 M BCB in: (A) ethaline + 0.5 M H_2SO_4; (B) ethaline + 0.5 M HNO_3; (C) ethaline + 0.5 M HCl; (D) ethaline + 0.5 M $HClO_4$; (E) 0.1 M KNO_3 + 0.1 M PB (pH 7.0).

w/v). For enzyme immobilization, 1 μL of the corresponding enzyme/BSA solution, mixed with 1 μL of GA (2.5% v/v) as cross-linking agent, was cast on the bare or modified electrodes and then left to react at room temperature during 1 h. After drying, the biosensors were immersed in PB solution (pH 7.0) for at least 2 h before use.

3. Results and discussion

3.1. Influence of the composition of the polymerization solution on PBCB film growth

Electrodeposition by potential cycling can be influenced by factors that include the composition of the supporting electrolyte, pH, monomer concentration, temperature, applied potential, scan rate, etc. Fig. 1A–E shows CVs for the electropolymerization of BCB on MWCNT/GCE from an ethaline-acid solution containing different acids as anion sources, H_2SO_4, HNO_3, HCl, $HClO_4$ and, for comparison, in 0.1 M PB (pH 7.0) + 0.1 M KNO_3 aqueous solution, at a scan rate of 50 mV s^{-1}. BCB species oxidise at high potentials (≈+0.80 V) and it has been proposed that the amino group oxidises to form a cation radical. The cation radicals are cross-linked by electropolymerization via a C–N coupling reaction forming stable PBCB [6,22]. Thus, in this work, the potential range was from - 0.6 V to +1.0 V vs. Ag/AgCl. In all polymerization media, the CV show an increase of the peak currents with increasing number of cycles indicating nucleation and growth processes [23].

For CV of PBCB electrodeposited on MWCNT/GCE in ethaline-acid, Fig. 1A–D, three redox couples marked as I_a/I_c, II_a/II_c and III_a/III_c appear. The I_a/I_c couple is assigned to the oxidation/reduction of the monomer units trapped in the polymer film and the other redox pairs are due to alternating oxidized and reduced repeat units in the polymer structure. The unpaired electrons can be localized at either the nitrogen atom or the other carbon atoms in the benzene ring. The cation radicals are more concentrated near the electrode surface; their diffusion rate is high, they may find a neutral monomer to react with or, more likely, they react with other radicals forming dimers and trimers. This new structure can undergo deprotonation and form intermediate polymerization products [24].

For BCB electropolymerised in aqueous solution, Fig. 1E, only two redox peaks are seen, I_a/I_c and II_a/II_c; the redox peaks I_a/I_c continuously decrease with the number of cycles while II_a/II_c increases and there is no formation of intermediates. Interestingly, the redox peaks of PBCB electrodeposited on MWCNT/GCE from ethaline-acidic media (pH 2.0) are at more positive potentials than those of PBCB electrodeposited in aqueous solution (pH 7.0). This means that the redox process is directly related with protons being

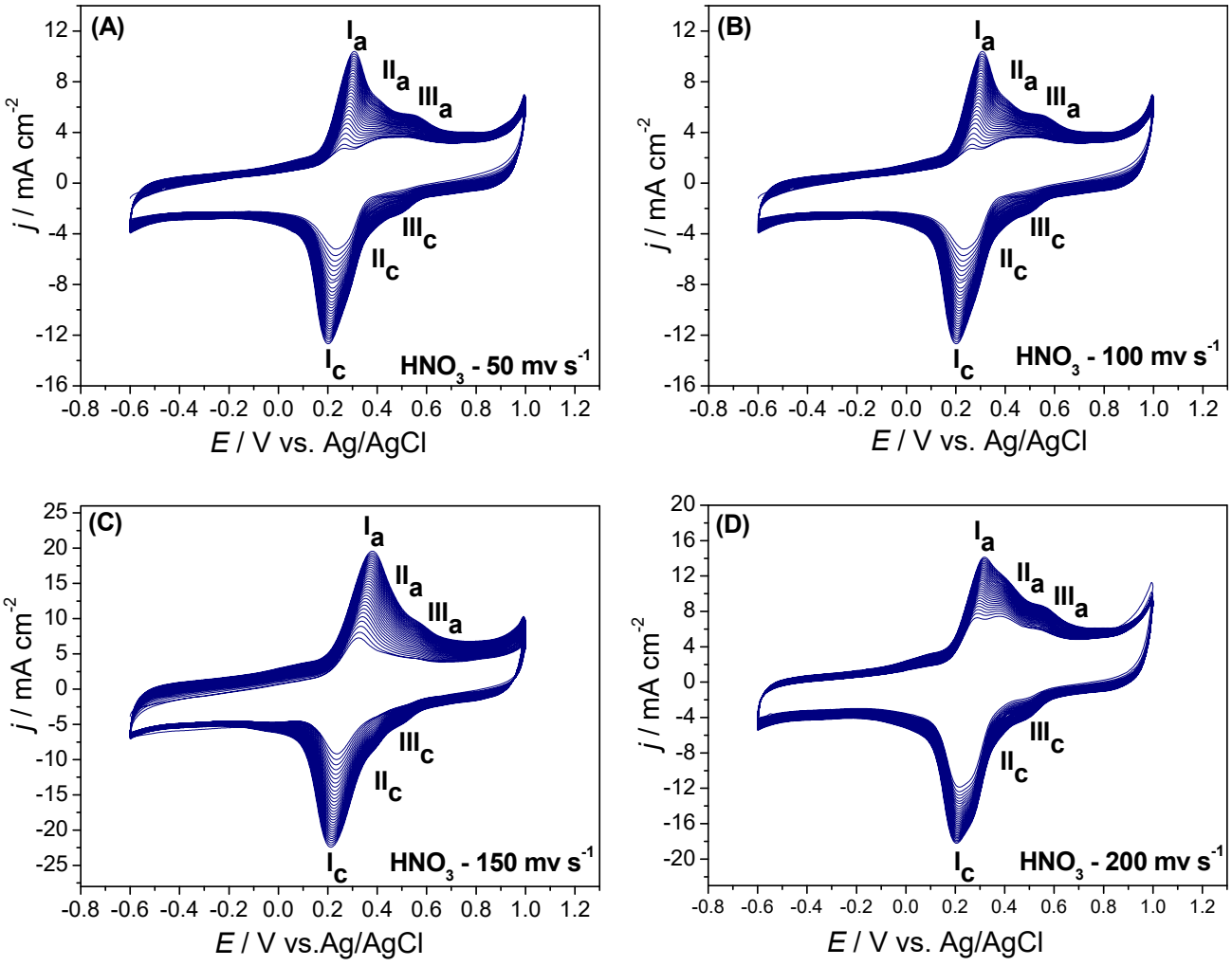

Fig. 2. Potential cycling electrodeposition of PBCB on MWCNT/GCE from a solution of 0.1 M BCB in ethaline +0.5 M HNO_3 at different scan rates: (A) 50; (B) 100; (C) 150; (D) 200 mV s^{-1}.

released into the solution from the polymer during its oxidation, and vice versa for reduction. This behaviour has also been found for other poly (azines) e.g., poly(methylene blue), poly(brilliant green), Poly(Nile blue), and polyaniline [11,25,26].

The mechanism of electropolymerization of BCB on MWCNT has been reported elsewhere in the literature [1,6,7]. The sidewall curvature of MWCNT, the π-π conjugative structure and highly hydrophobic surface, allow them to interact with BCB monomer, through π-π interactions and/or hydrophobic interactions. Electrostatic interactions can also occur at sufficiently high pH, due to carboxylate groups at the defects and extremities of the functionalized MWCNT attracting the positively charged amino groups of BCB. In the acidic polymerization media used here, the former mechanism will take place.

The formal potential ($E^0 = (E_{pa} + E_{pc})/2$) of the monomer units within the polymer film structure was calculated from the redox couple I_a/I_c, in the CVs obtained at 50 mV s^{-1} scan rate. The formal potential was calculated for the 1st cycle and 30th cycle, and the values were, vs. Ag/AgCl:

$PBCB_{Ethaline}$-H_2SO_4/MWCNT/GCE: $E^0_1 = 0.24$ V and $E^0_{30} = 0.26$ V;

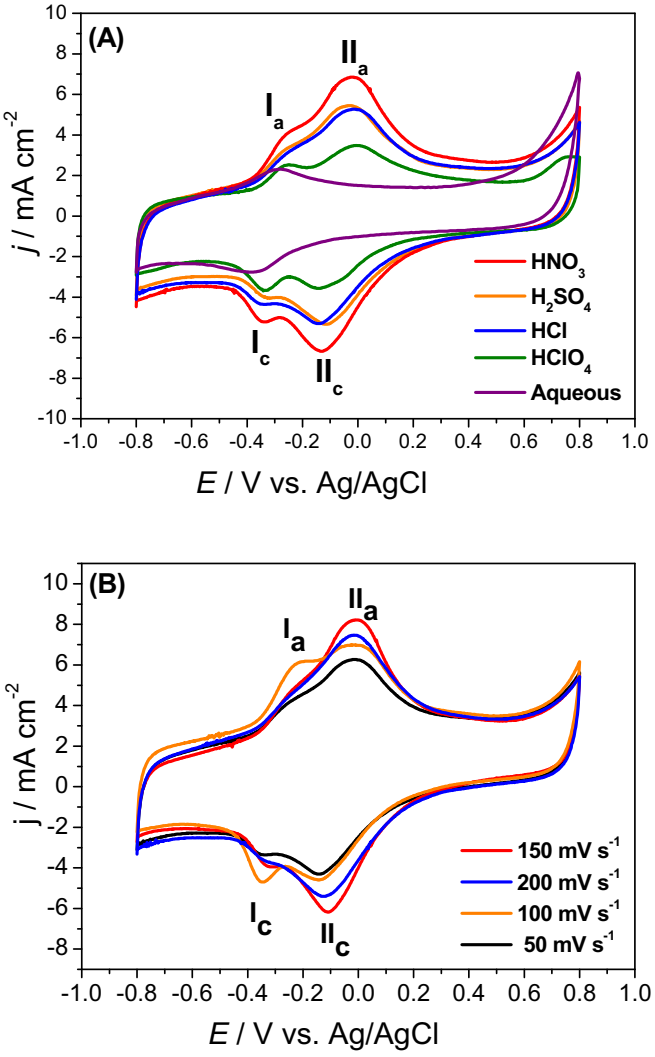

Fig. 3. (A) CVs of $PBCB_{Ethaline\text{-}acid}$ modified MWCNT/GCE in 0.1 M BR buffer solution (pH 7.0) at 50 mVs^{-1}; (B) CVs of $PBCB_{Ethaline}$-HNO_3 modified MWCNT/GCE, for PBCB films formed at different scan rates: from 50 to 200 mV s^{-1} in 0.1 M BR buffer solution (pH 7.0) at 50 mV s^{-1}.

$PBCB_{Ethaline}$-HCl/MWCNT/GCE: $E^0_1 = 0.25$ V and $E^0_{30} = 0.27$ V;
$PBCB_{Ethaline}$-HNO_3/MWCNT/GCE: $E^0_1 = 0.25$ V and $E^0_{30} = 0.27$ V;
$PBCB_{Ethaline}$-$HClO_4$/MWCNT/GCE: $E^0_1 = 0.15$ V and $E^0_{30} = 0.16$ V;
$PBCB_{aqueous}$/MWCNT/GCE: $E^0_1 = -0.084$ V and $E^0_{30} = -0.073$ V.

Only very small differences in the values of the formal potential of PBCB electrodeposited in the presence of ethaline with different acids are seen, except for $HClO_4$. The large difference in the formal potentials for PBCB electrodeposited from aqueous solution compared with PBCB electrodeposited from ethaline is due to the higher pH. Very little change in the E^0 values occurs during polymer growth.

The polymer growth rate expressed as the ratio between the oxidation peak current in the thirtieth and in the first cycle I_{a30}/I_{a1} was calculated. For $PBCB_{Ethaline}$-H_2SO_4/MWCNT/GCE is 10.0, for $PBCB_{Ethaline}$-HCl/MWCNT/GCE is 7.3, for $PBCB_{Ethaline}$-HNO_3/MWCNT/GCE is 11.7, for $PBCB_{Ethaline}$-$HClO_4$/MWCNT/GCE is 3.2 and for $PBCB_{aqueous}$/MWCNT/GCE, is 3.9. From this point of view, HNO_3 is the best acid dopant, closely followed by H_2SO_4. It was previously observed [4,27] that NO_3^- acts as a polymerization accelerator and it can also serve as a shielding agent since it neutralizes the positive charge of BCB molecules. On the other hand, some other anions (ClO_4^-, BF_4^-) are known to form tight ionic pairs with BCB^+, precipitating the BCB monomer and/or produce polymer films with an irregular nanostructure [4,27], see Fig. 5F.

3.2. Influence of the scan rate on PBCB film growth

The influence of scan rate on BCB electropolymerization in the range 50–200 mV $s^{-1}$was investigated in ethaline + HNO_3 solution since, in this medium, PBCB exhibited the best growth profile, Fig. 2A–D. The peak currents corresponding to the polymer redox processes increased with increase of scan rate from 50 to 150 mV s^{-1}, but decreased at 200 mV s^{-1}; this is in agreement with previous observations for poly(methylene blue) in Ref. [28]. This behaviour may be explained as follows. The scan rate during polymerization influences the mass transport of the monomer from the solution to the electrode, as does the viscosity of the solution. In viscous solutions ion movement is more difficult, but an increase in scan rate will increase diffusion of the monomer in the solution towards the electrode surface owing to the concentration gradient created by its oxidation. However, at higher scan rates, the monomer cannot be replenished at the electrode surface sufficiently fast, due to the high viscosity, so that a decrease in monomer oxidation current will be observed. This will limit polymer growth and the effect is already seen at 200 mV s^{-1} scan rate. The formal potential is not influenced by the scan rate, being $E^0_1 = 0.25 \pm 0.02$ V and $E^0_{30} = 0.27 \pm 0.02$ V. The polymerization growth rate for different scan rates (cycle 30 divided by cycle 1 peak current) was calculated as 11.7, 11.9, 12.5 and 6.4 for 50, 100, 150 and 200 mV s^{-1}, respectively. Thus, among the scan rates investigated for polymer growth, the best was 150 mV s^{-1}, in agreement with results in Ref. [28].

3.3. Electrochemical properties of the nanocomposite films

3.3.1. Cyclic voltammetry

In order to evaluate the electrochemical behaviour of PBCB on MWCNT with a view to applications, CVs of the modified electrodes were recorded in 0.1 M BR buffer solution (pH 7.0) at a potential scan rate of 50 mV s^{-1}. Fig. 3A displays CVs of the PBCB/MWCNT nanocomposite films formed in the various media described in the previous sections. The CV profiles of PBCB electrodeposited in ethaline containing different acids show the same two redox couples, a less well-defined I_a/I_c attributed to entrapped BCB monomer and a well-defined II_a/II_c corresponding to the polymer film, while

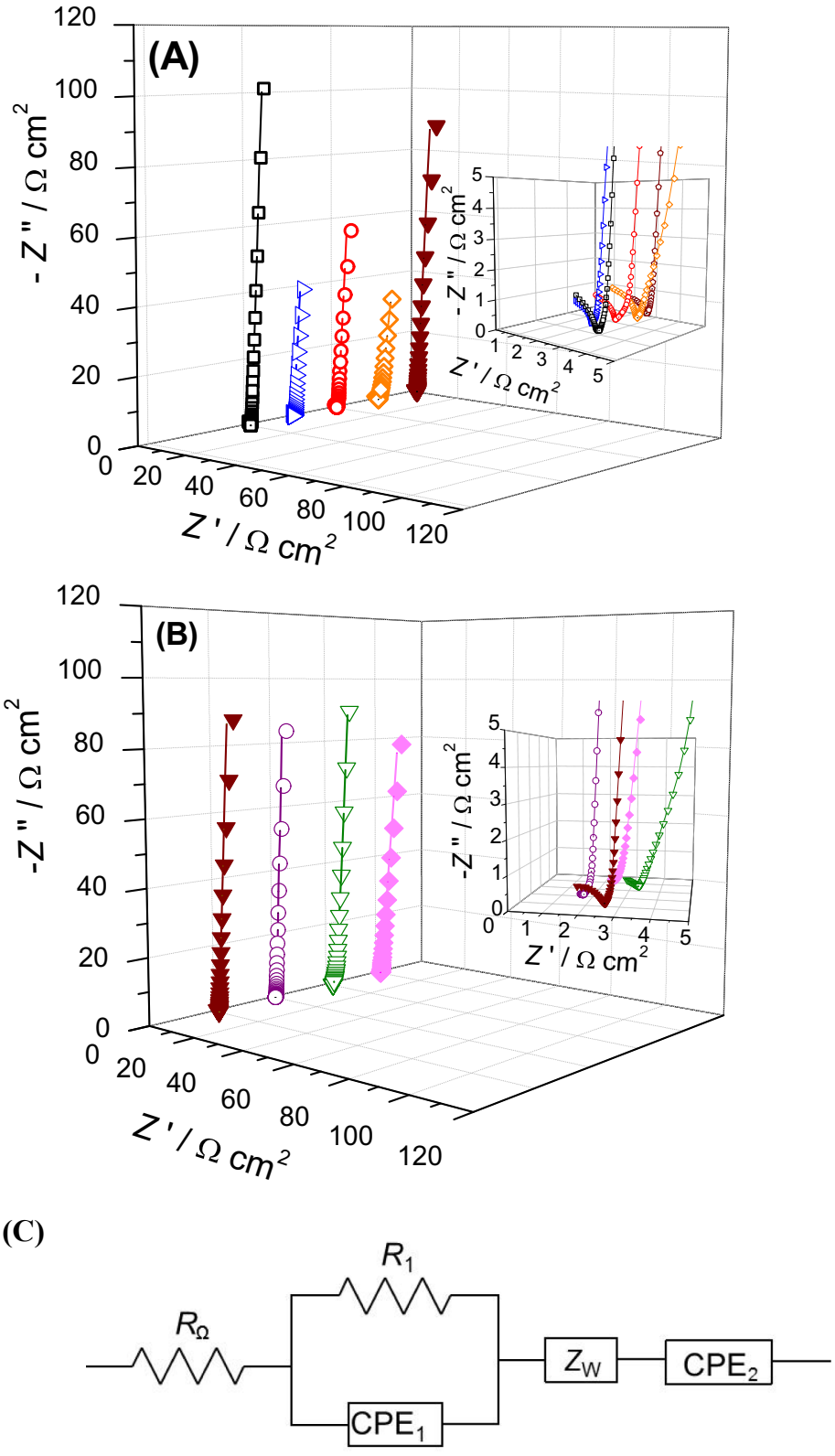

Fig. 4. Complex plane impedance spectra at PBCB/MWCNT/GCE in 0.1 M BR buffer solution (pH 7.0), PBCB film synthesized (A) at 50 mV s^{-1} in (□) 0.1 M KNO_3 + 0.1 M PB solution (pH 7.0); (▶) ethaline + 0.5 M H_2SO_4; (◯) ethaline + 0.5 M HCl; (◇) ethaline + 0.5 M $HClO_4$; (▼) ethaline + 0.5 M HNO_3, (B) in ethaline + 0.5 M HNO_3 at scan rates: (□) 50; (▽) 100; (◯) 150 and (◆) 200 mV s^{-1}. (E) Equivalent electrical circuit used to fit the spectra.

PBCB electrodeposited in aqueous solution presents just one redox couple I_a/I_c shifted to more negative potentials; the same tendency was also verified during electropolymerization. The CVs clearly evidence that PBCB films obtained in ethaline containing different acids have higher peak currents, which may be attributed to a greater amount of polymer electrodeposited than that of PBCB formed in aqueous solution. The peak-to-peak separation ($\Delta E_p = E_{pa}$ - E_{pc}) was calculated to be 0.08 V in aqueous solution and ~0.13 V in ethaline-acid media. The surface coverage (Γ) of the nanocomposites was estimated using the equation [29]:

$$\Gamma = /nFA \quad (1)$$

where Γ is the surface concentration (mol cm^{-2}), is the charge(C)

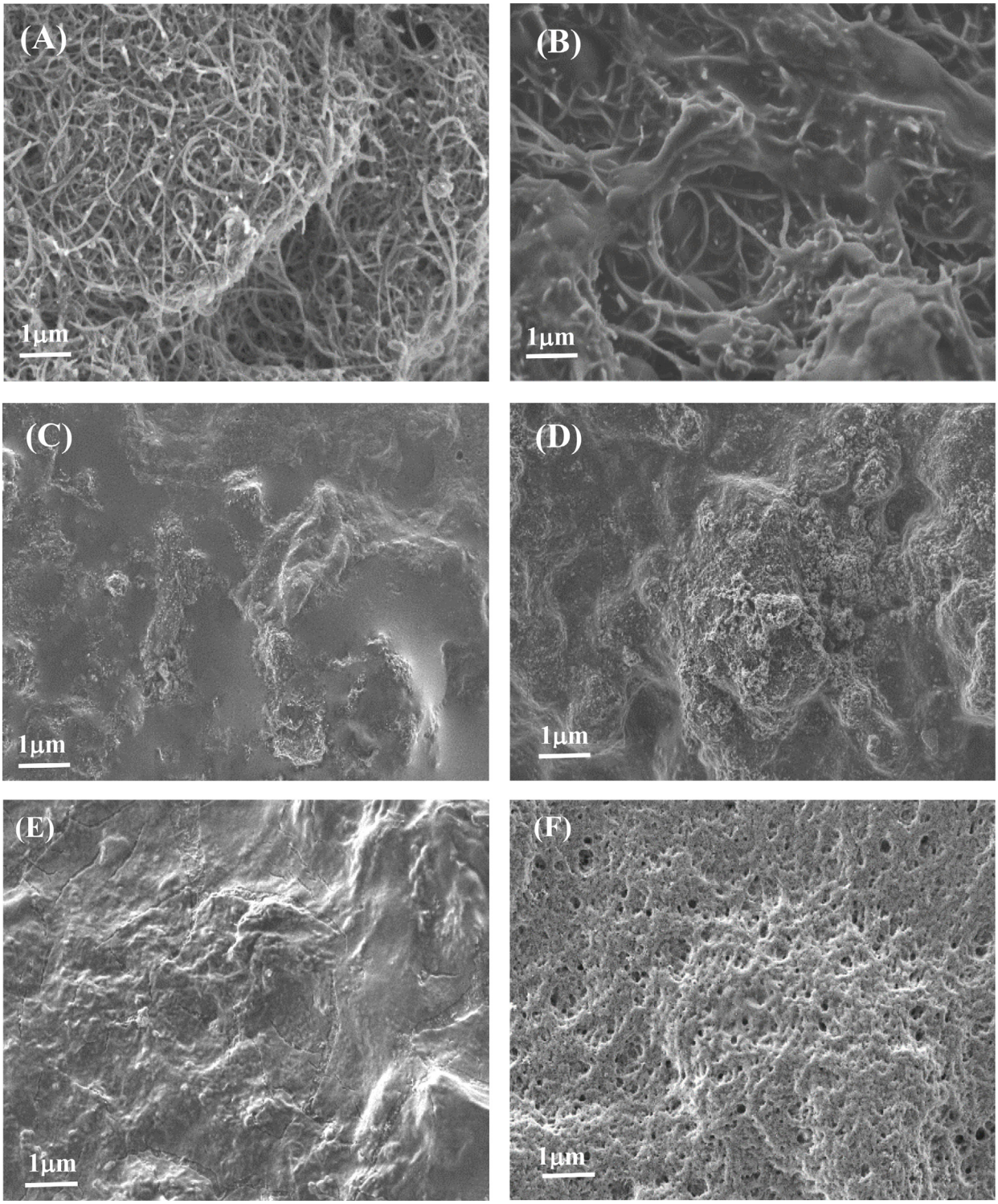

Fig. 5. SEM micrographs on carbon film electrodes of (A) Multiwalled-carbon nanotubes (MWCNT); (B) $PBCB_{aqueous}$/MWCNT nanocomposite film; (C) $PBCB_{Ethaline}$-HNO_3/MWCNT nanocomposite film; (D) $PBCB_{Ethaline}$-H_2SO_4/MWCNT nanocomposite film; (E) $PBCB_{Ethaline}$-HCl/MWCNT nanocomposite film; (F) $PBCB_{Ethaline}$-$HClO_4$/MWCNT nanocomposite film.

obtained by integrating the corresponding area of the cathodic peak II_c; after baseline correction, n (=2) is the number of electrons transferred (calculated in Section 3.5), F is the Faraday constant (96485 C mol^{-1}) and A is the electrode geometric surface area (0.00785 cm^2). The calculated order of increasing Γ values was $9.31 \times 10^{-8} < 1.04 \times 10^{-7} < 1.93 \times 10^{-7} < 2.31 \times 10^{-7} < 4.27 \times 10^{-7}$ mol cm^{-2}, for $PBCB_{aqueous}$/MWCNT, $PBCB_{Ethaline}$-$HClO_4$/MWCNT, $PBCB_{Ethaline}$-HCl/MWCNT, $PBCB_{Ethaline}$-H_2SO_4/MWCNT and $PBCB_{Ethaline}$-HNO_3/MWCNT modified GCE, respectively. The order of these values is in agreement with what is observed in Fig. 1, in which the BCB polymerized in ethaline containing NO_3^- presented the highest increase in current during polymerization. Fig. 3B shows CVs for $PBCB_{Ethaline}$-$HClO_4$/MWCNT/GCE with PBCB electrodeposited at different scan rates from 50 to 200 mV s^{-1}. As expected, the peak currents increased with increase of electropolymerization scan rate up to 150 mV s^{-1}, where the highest peak current was achieved, decreasing for 200 mV s^{-1}.

The values of ΔE_p for $PBCB_{Ethaline}$-HNO_3 films were 0.133 V, 0.113 V, 0.102 V and 0.110 V for films electrodeposited at 50, 100, 150 and 200 mV s^{-1}. Mirroring the trend in polymer film growth, the ΔE_p values decrease with increasing scan rate up to 150 mV s^{-1}. The surface coverage (Γ) was estimated to be $4.27 \times 10^{-7} < 4.84 \times 10^{-7} < 5.74 \times 10^{-7} > 5.05 \times 10^{-7}$ mol cm^{-2}, for $PBCB_{Ethaline}$-HNO_3 electrodeposited at 50, 100, 150 and 200 mV s^{-1}, respectively. Therefore, the electropolymerization of BCB in ethaline containing NO_3^- at 150 mV s^{-1} scan rate led to the formation of polymer/MWCNT structures with the best electrochemical properties.

3.3.2. Electrochemical impedance spectroscopy

Electrochemical impedance spectroscopy was used to examine the interfacial properties of the PBCB films electrodeposited under different experimental conditions. The measurements were carried out at an applied potential of - 0.10 V vs. Ag/AgCl, chosen from cyclic voltammograms recorded at the modified electrodes, Fig. 3A, corresponding to the approximate formal potential value for oxidation/reduction of the polymer, peaks II_a/II_c. BR buffer solution (0.10 M, pH 7.0) was used as supporting electrolyte, the same as for characterization by cyclic voltammetry.

In all cases, the spectra obtained present three regions: a semicircular part at high frequencies corresponding to the electron transfer processes and two linear parts at medium and lower frequencies corresponding to diffusional and charge separation phenomena, respectively. The spectra in the low-frequency region are very similar for all types of modified electrode, the main differences only appearing in the high-frequency region.

Complex plane impedance spectra are illustrated in Fig. 4A, for PBCB polymer films obtained from ethaline + different acids (H_2SO_4, HNO_3, HCl and $HClO_4$) and from aqueous solution (PB+KNO_3), and Fig. 4B are spectra of PBCB films obtained at different scan rates (50, 100, 150 and 200 mV s^{-1}). The spectra were all fitted to the electrical circuit depicted in Fig. 4C. The circuit comprises a cell resistance, R_Ω, in series with a parallel combination of a resistance R_1 and CPE_1 which is modelled as non-ideal capacitor expressed by $CPE = 1/(i\omega C)^\alpha$, where C is the capacitance, ω is the frequency in rad s^{-1} and the exponent, $0.5 < \alpha < 1$, reflects the surface non-uniformity and roughness of the modified electrodes, $\alpha = 1$ corresponding to a perfect uniform and smooth surface [30]. The constant phase element (CPE_1) and the resistance (R_1) are associated with the processes which occur at the electrode/modifier interface at high frequencies. The intermediate frequency region is modelled by a mass transport finite-diffusion Warburg element Z_W. The Warburg element, Z_w, results from the equation: $Z_w = R_D \text{cth}\,[\tau i\omega)^\alpha] \times [\tau i\omega)^\alpha]$, where $\alpha < 0.5$, and is characterized by a diffusional time constant (τ), a diffusional pseudocapacitance (C_D) and a diffusional resistance ($R_D = \tau/C_D$) [30]. For low frequencies a second constant phase element was used, CPE_2, corresponding to the charge separation at the modifier film/solution interface and within the film. Values of the circuit parameters obtained by fitting the spectra are presented in Table 1.

The charge separation processes occurring at the electrode/modifier interface are influenced by the nanocomposite structures, reflected by the different values of CPE_1 obtained. For all PBCB polymer films prepared in ethaline, there is a decrease in R_1 values accompanied by an increase in C_1, attributed to greater charge separation, and easier electron transfer compared with PBCB films produced in aqueous solution. Values of R_1 decrease in the order: ($PBCB_{aqueous}$/MWCNT/GCE) > ($PBCB_{Ethaline}$-$HClO_4$/MWCNT/GCE) > ($PBCB_{Ethaline}$-HCl/MWCNT/GCE) > ($PBCB_{Ethaline}$-H_2SO_4/MWCNT/GCE) > ($PBCB_{Ethaline}$-HNO_3/MWCNT/GCE), the fastest electron transfer occurring at $PBCB_{Ethaline}$-HNO_3/MWCNT/GCE. The average $\alpha_1 \approx 0.85$, for films obtained in ethaline, reflects a relatively high surface uniformity of the polymer films at the nanometric scale. For PBCB films formed in aqueous solution, α_1 was 0.77, revealing a less smooth film, as also verified in SEM analysis, see below. The values of R_1 for $PBCB_{Ethaline}$-HNO_3/MWCNT/GCE obtained at different electropolymerization scan rates were in the order: 50 mV s^{-1} > 100 mV s^{-1} > 200 mV s^{-1} > 150 mV s^{-1}. Values of CPE_1 also show a scan rate dependence, in the inverse sense, with films prepared at 150 mV s^{-1} giving the highest charge separation. This is in agreement with the CV results.

The values of diffusional resistance obtained from the Warburg element increased at polymer films electrodeposited in ethaline compared with those in aqueous solution, spectra in Fig. 4A, which may be attributed to a thicker film, as also observed from the values of τ, which were also a bit higher. The exponent α calculated from the Warburg element was close to 0.45, as usually found in thin films [31]. From fitting the spectra in Fig. 4B, the scan rate seems to

Table 1
Equivalent circuit element values obtained by fitting the impedance spectra in Fig. 4A (polymerization scan rate 50 mV s^{-1}) and 4B (different scan rates in Eth + HNO_3). Eth: ethaline.

Experimental conditions	R_1/Ω cm^2	CPE_1/(μF cm^{-2} s$^{\alpha-1}$)	α_1	Z_w/Ω cm^2	τ/ms	α_{zw}	CPE_2/(mF cm^{-2} s$^{\alpha-1}$)	α_2	Error[a] (%)
Aqueous	5.98	12.5	0.77	1.01	0.07	0.46	68.5	0.80	4.3
Eth + $HClO_4$	3.63	21.1	0.84	1.72	0.71	0.49	98.3	0.85	4.7
Eth + HCl	2.10	57.1	0.86	1.71	0.75	0.49	132.2	0.84	4.5
Eth + H_2SO_4	1.73	66.3	0.88	1.74	0.76	0.48	148.2	0.95	4.6
Eth + HNO_3	1.15	94.1	0.85	1.63	0.78	0.49	198.4	0.96	4.5
Scan rate/mV s^{-1}									
50	1.15	94.1	0.85	1.63	0.78	0.49	198.4	0.96	4.5
100	0.87	118.2	0.86	1.76	0.76	0.50	220.4	0.92	4.3
150	0.12	155.3	0.84	1.80	0.84	0.49	268.1	0.97	4.7
200	0.38	125.2	0.85	1.79	0.80	0.49	232.4	0.95	4.6

[a] Error calculated by ZView software.

have little influence on diffusional resistance values.

In relation to CPE_2, the trend is the same as for CPE_1. Varying the acid dopant significantly influences the values, being highest for HNO_3, and the values of α_2 also increase, being very similar for H_2SO_4 and HNO_3 dopants. There is not much influence of scan rate on CPE_2 or the α_2 values.

3.4. Morphological characterization of the nanostructured films

The morphology of the nanostructured PBCB films electrodeposited in ethaline in the presence of different acids as anion source and in aqueous solution was examined by SEM, see Fig. 5. SEM images of MWCNT without, Fig. 5A, and with polymer electrodeposited, Fig. 5B–F were recorded. Fig. 5A shows the MWCNT morphology prior to polymer deposition, with the presence of agglomerates of MWCNT entangled bundles, of uniform diameter and smooth surface, and without any indication of metallic catalysts obtained from their synthesis, which indicates the success of the acid treatment.

An SEM image of PBCB electrodeposited on MWCNT in aqueous solution is shown in Fig. 5B. The diameter of the MWCNT increases after deposition of the $PBCB_{aqueous}$ film, as observed by comparing the SEM images before and after PBCB electrodeposition. However, a non-uniform and very thin film is formed, that is, BCB polymerization from aqueous solution did not change the overall morphology of the MWCNT surface revealed by the presence of some exposed MWCNT bundles in the composite film, as also reported in Refs. [32–34] for other poly(azines) synthesized in aqueous solution. Fig. 5C–F shows the morphology of PBCB films electrodeposited in ethaline DES in the presence of different acids as anion source, namely HNO_3, H_2SO_4, HCl, and $HClO_4$. In contrast to aqueous solution, the use of DES for BCB polymerization shows the formation of rough and compact nanostructures covering all the MWCNT bundles for all four systems evaluated. This can explain their enhanced electrochemical properties, namely the higher polymer oxidation and reduction currents in CVs and the lower charge transfer resistance in EIS compared with PBCB synthesized in aqueous solution, Fig. 3A and Table 1.

Furthermore, the use of different anion sources played an important role in the nanocomposite film morphology. PBCB $_{Ethaline}$-HNO_3/MWCNT presents a more uniform surface than the other nanocomposite films that may explain the best electrochemical performance. PBCB $_{Ethaline}$-H_2SO_4/MWCNT nanocomposite film reveals the presence of a thicker film and less uniform surface with the presence of agglomerates. $PBCB_{Ethaline}$-HCl/MWCNT nanocomposite film has a relatively smooth surface but appears brittle, that may be responsible for its lower stability and less good electrochemical performance than $PBCB_{Ethaline}$-HNO_3/MWCNT and $PBCB_{Ethaline}$-H_2SO_4/MWCNT. $PBCB_{Ethaline}$-$HClO_4$/MWCNT presents an irregular sponge-like surface, which may be due to a change in the mechanism of polymer deposition in the presence of ClO_4^- that, during the initial formation of the polymer film, hinders direct access of unreacted monomers to the electrode surface leading to formation of an irregular, thinner and less conductive film than the other polymer films prepared in ethaline [35].

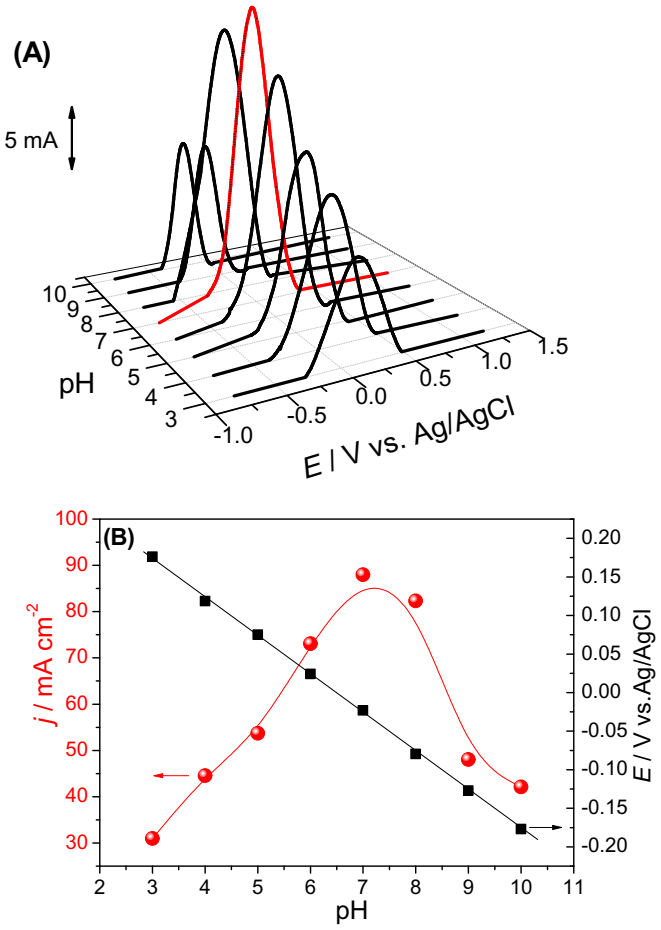

Fig. 6. (A) Differential pulse voltammograms at $PBCB_{Ethaline}$-HNO_3/MWCNT film modified electrodes in BR buffer solution at different pH values (from 3.0 to 10), recorded at 50 mV s^{-1}(B) plots of oxidation peak currents and peak potentials vs. pH, data from Fig. 6A.

3.5. Effect of pH on peak current and peak potential at the modified electrodes

Due to the presence of amino groups in poly(azines), protons are involved in the electrode reactions. Hence, the effect of solution pH at $PBCB_{Ethaline}$-HNO_3/MWCNT/GCE, with PBCB electrodeposited at 150 mV s^{-1}, was investigated by differential pulse voltammetry (DPV) in 0.1 M BR buffer solution in the pH ranging from 3.0 to 10.0. The parameters used in DPV were: amplitude 10 mV, step potential 2 mV, scan rate 50 mV s^{-1} and pulse time 10 ms. As seen in Fig. 6A, with increase in pH, the oxidation peak potential (E_{pa}) shifts linearly to negative potentials, according to the equation: E_{pa}/V = 0.32–0.056 pH, the slope of ≅ 56 mV pH^{-1}, Fig. 6B, indicating an equal number of protons and electrons participating in the oxidation process. DPV also demonstrated that the peak current increases with increase in pH up to pH 7.0, where the highest response is exhibited, and then decreases. Therefore, this pH was selected for further experiments. The peak width at half-height ($W_{1/2}$) gives an indication of the reversibility of electrode reaction and the number of electrons involved. The value of $W_{1/2}$ in pH 7.0 BR buffer solution was estimated to be 42 ± 3 mV (three measurements), suggesting that the total number of electrons transferred in the oxidation of the electroactive centres in the polymer is equal to 2, together with 2 protons. There are contradictory reports in the literature regarding the number of electrons involved in BCB oxidation, the number seeming to be dependent on the electrode support material and experimental conditions. It was found that the electron transfer is a one electron process in Refs. [4,36], but a 2 electron process in Refs. [7,21,37], in agreement with what was obtained here.

3.6. Effect of the scan rate at modified electrodes

The effect of the scan rate in 0.1 M BR buffer solution, pH 7.0 was

investigated at $PBCB_{Ethaline}$-HNO_3/MWCNT/GCE with PBCB films electrodeposited at different scan rates namely, 50, 100, 150 and 200 mV s^{-1} and with $PBCB_{aqueous}$/MWCNT film electrodeposited at 150 mV s^{-1}. The anodic and cathodic peak currents increase with increase of scan rate from 10 to 100 mV s^{-1}, as illustrated in Fig. 7A for the $PBCB_{Ethaline}$-HNO_3/MWCNT/GCE with film electrodeposited at 150 mV s^{-1}, and which exhibited the highest peak currents. For all nanocomposite films, there is a linear relationship between the anodic peak current, I_{pa} and the cathodic peak current, $I_{pc,}$ with scan rate, v, Fig. 7B, as also observed in Refs. [36,37] for other PBCB modified electrodes. The following equations were obtained: for the redox couple (I_a/I_b) $j_{pIa} = 0.006 + 0.26\ v$ and $j_{pIb} = 0.007-0.32\ v$ and for the redox couple (II_a/II_b) $j_{pIIa} = 0.05 + 42.1\ v$ and $j_{pIIb} = -0.23-31.2\ v$, where the current densities (j) are expressed in mA cm^{-2} and the scan rates (v) are in V s^{-1}.

The relationship log (j_{pIIa}/mA cm^{-2}) vs log (v/V s^{-1}) (not shown) was plotted for all modified electrodes. The slopes (S) were calculated to be 0.98, for $PBCB_{aqueous}$/MWCNT/GCE at 150 mV s^{-1}, for $PBCB_{Ethaline}$-HNO_3/MWCNT/GCE the values were 0.96 (50 mV s^{-1}); 0.96 (100 mV s^{-1}), 0.97 (150 mV s^{-1}) and 0.96 (200 mV s^{-1}), all close to the theoretical value of 1.0, characteristic of a surface-confined process [38].

3.7. Application of the $PBCB_{Ethaline}$-HNO_3/MWCNT nanocomposite film in enzyme biosensors

After optimization of the best conditions for PBCB electrodeposition in DES and corresponding film characterization, application of the nanocomposite-modified electrode (with BCB electropolymerised at scan rate 150 mV s^{-1}) in enzyme biosensors was investigated. Fixed potential amperometry was carried out by successive addition of glucose or catechol aliquots in buffer and the corresponding enzyme (GOx or Tyr immobilized on $PBCB_{Ethaline}$-HNO_3/MWCNT/GCE) catalysed response measured, see Fig. 8A1 and 8B1, respectively. For comparison, the enzymes were also immobilized on $PBCB_{aqueous}$/MWCNT/GCE and unmodified GCE, as described in the experimental section. All experiments were repeated three times; each set of measurements consists in 16 successive analyte injections. No enzyme leaching from the electrode was observed after these measurements.

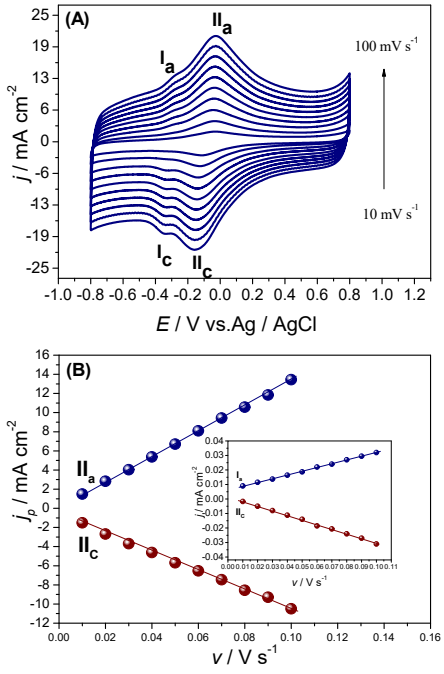

Fig. 7. (A) CVs for $PBCB_{Ethaline}$-HNO_3/MWCNT modified GCE in 0.1 M BR buffer solution (pH 7.0) at scan rates 10–100 mV s^{-1}; (B) Plots of peak current vs. scan rate.

3.7.1. Determination of glucose

Fig 8A2 displays calibration plots at the glucose oxidase biosensors following sequential additions of glucose under continuous stirring at an applied potential of - 0.3 V vs. Ag/AgCl in 0.1 M PB solution (pH 7.0), as in Ref. [39].

In order to compare the sensitivity of the three biosensor configurations GOx/$PBCB_{Ethaline}$-HNO_3/MWCNT/GCE, GOx/$PBCB_{aqueous}$/MWCNT/GCE and GOx/GCE, the same amount of glucose oxidase was immobilized on all electrodes, see details in experimental section.

The first biosensor assembly, with PBCB deposited in DES, exhibited the highest sensitivity of 700 μA cm^{-2} mM^{-1} and the lowest limit of detection of 2.9 μM. The second, with PBCB deposited in aqueous solution, had a 30% lower sensitivity of 500 μA cm^{-2} mM^{-1} and higher limit of detection of 4.2 μM. GOx/GCE showed significantly inferior analytical parameters: a sensitivity of 5.0 μA cm^{-2} mM^{-1} and limit of detection of 12.1 μM. The apparent Michaelis-Menten constant, K_M, is the concentration corresponding to half the maximum, saturation response of the biosensor. K_M can be estimated as around 80 μM for the first two biosensor assemblies with PBCB and around 400 μM for the GCE without it.

Comparison of the analytical parameters of GOx/$PBCB_{Ethaline}$-HNO_3/MWCNT/GCE with the most recent glucose oxidase-based electrochemical biosensors was made. The novel approach offers better characteristics (limit of detection and sensitivity) than other glucose biosensors recently reported in the literature. For example, when GOx was adsorbed onto a nanoporous TiO_2 film layer on the surface of an iron phthalocyanine (FePc) vertically-aligned CNT-modified electrode, the biosensor exhibited a sensitivity of only 8.25 μA cm^{-2} mM^{-1}, the linear range was from 50 μM to 4.0 mM and a much higher detection limit of 30 μM [40]. Mani et al. [41] developed a biosensor for glucose, by immobilization of GOx on electrochemically reduced graphene oxide–MWCNT hybrid modified glassy carbon electrode (GCE); the sensitivity of this biosensor was 7.95 μA cm^{-2} mM^{-1}, the linear range was 10 μM–6.5 mM and the limit of detection was 4.70 μM. Luo et al. [42] also proposed a glucose biosensor, by immobilization of GOx on a reduced graphene oxide/PAMAM–silver nanoparticles nanocomposite (RGO–PAMAM–Ag), the sensitivity being 75.75 μA cm^{-2} mM^{-1}, the linear range was between 320 μM and 6.5 mM and the limit of detection 4.50 μM, higher than in this work.

3.7.2. Determination of catechol

The same platforms were used to prepare Tyr biosensors for the amperometric detection of catechol. Amperometric measurements were carried out in 0.1 M PB solution (pH 7.0), at an applied potential of −0.2 V vs.Ag/AgCl, as in Ref. [43]. Aliquots of catechol solution were injected into the electrochemical cell under stirring, as for glucose. Fig. 8B2 shows the corresponding calibration plots. The Tyr/$PBCB_{Ethaline}$-HNO_3/MWCNT/GCE presented the best performance for catechol determination, as occurred for glucose with GOx, with the highest sensitivity of 750 μA cm^{-2} mM^{-1} and lowest limit of detection of 3.9 μM. The Tyr/$PBCB_{aqueous}$/MWCNT/GCE biosensor exhibited a sensitivity of 330 μA cm^{-2} mM^{-1} and a limit of detection of 5.3 μM whereas Tyr/GCE presented a sensitivity of 30 μA cm^{-2} mM^{-1} and a limit of detection of 43 μM. The values of K_M, are around 80 μM for the first two biosensor assemblies with PBCB and around 1000 μM for GCE without PBCB. The analytical parameters of the Tyr/$PBCB_{Ethaline}$-HNO_3/MWCNT/GCE biosensor

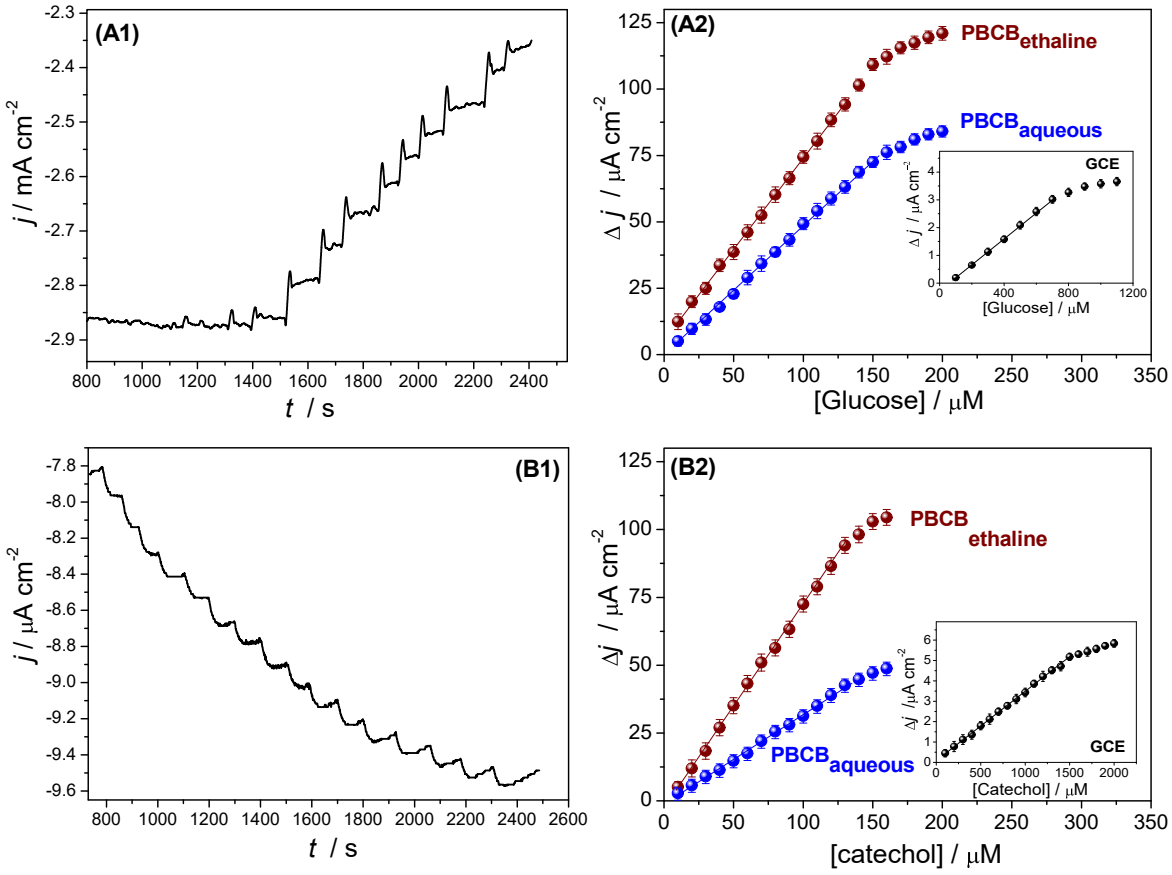

Fig. 8. Amperometric response of (A1) GOx/PBCB$_{ethaline}$/MWCNT/GCE biosensor to glucose response and (B1) Tyr/PBCB$_{ethaline}$/MWCNT/GCE biosensor to catechol in PB (pH 7.0) at applied potential of −0.3 V and −0.2 V vs. Ag/AgCl, respectively. Calibration plots for enzyme biosensors with enzyme immobilized on PBCB$_{ethaline}$ and PBCB$_{aqueous}$ modified MWCNT/GCE, (inset bare GCE) for (A2) glucose using GOx and (B2) catechol using Tyr.

were also compared with the most recent biosensors reported in the literature. Tembe et al. [44] developed an electrochemical biosensor for catechol using tyrosinase enzyme entrapped in an agarose–guar gum composite matrix with sensitivity 1 μA cm^{-2} mM^{-1}, the linear range was 65 μM–1.0 mM and a limit of detection of 6 μM. López and Ruiz [45] proposed a biosensor based on the immobilization of Tyr onto microparticles prepared by polymerization of the ionic liquid 1-vinyl-3-ethyl-imidazolium bromide (ViEtIm^{+}Br^{-}) for catechol determination having a sensitivity of 17.96 μA cm^{-2} mM^{-1}, the linear range was from 39 μM to 2.5 mM and a limit of detection of 20 μM. López and Merkoçi [46] also developed a biosensor for catechol determination using Tyr immobilized on MWCNT decorated by magnetic nanoparticles modified screen-printed electrode with a sensitivity of 4.8 μA cm^{-2} mM^{-1}, the linear range was between 10 μM–120 μM and limit of detection of 7.61 μM.

Additional experiments were performed, in order to evaluate if the absence of oxygen influences the electroactivity of the PBCB$_{Ethaline}$-HNO$_3$/MWCNT for both GOx and Tyr for glucose and catechol biosensing. Cyclic voltammograms were recorded in the presence and absence of oxygen, and no significant changes were observed, either in the voltammograms shape, or in the peak current. Compared with other sensors used for biosensing glucose and catechol, the proposed platform exhibited the lowest limit of detection, highest sensitivity and comparable linear range. These results also suggest that the novel PBCB$_{Ethaline}$-HNO$_3$/MWCNT platform has the best affinity for enzyme immobilization, presenting an excellent performance for enzyme electrochemical biosensors.

4. Conclusions

Brilliant cresyl blue has been successfully polymerized in ethaline-DES in the presence of a small amount of acid dopant, presenting superior properties compared with polymer films synthesized in aqueous solution. The composition of ethaline-acid solutions had an important role in PBCB growth also influencing their nanoscale morphology, and thence electrochemical behaviour. The polymer films electrodeposited in ethaline-HNO$_3$ presented a more uniform morphology and better electrochemical performance than with the other acids studied. The influence of scan rate is also an important factor in polymer electrodeposition, PBCB$_{Ethaline}$ electrodeposited at 150 mV s^{-1} exhibiting the best electrochemical characteristics. The enzymes GOx and Tyr were immobilized on PBCB $_{Ethaline}$-HNO$_3$/MWCNT/GCE, presenting excellent sensing performance for glucose and catechol determination. These properties demonstrate that the novel nanocomposite film modified electrode is very promising for future applications in electrochemical enzyme biosensors.

Acknowledgements

The authors thank Fundação para a Ciência e a Tecnologia (FCT), Portugal, projects PTDC/QEQ-QAN/2201/2014, in the framework of Project 3599-PPCDT, and UID/EMS/00285/2013 (both co-financed by the European Community Fund FEDER). WS thanks the

Conselho Nacional de Desenvolvimento Científico e Tecnológico (CNPq), Brazil for a doctoral fellowship, 232979/2014-6, and MEG thanks FCT for a postdoctoral fellowship SFRH/BPD/103103/2014.

References

[1] M.M. Barsan, M.E. Ghica, C.M.A. Brett, Electrochemical sensors and biosensors based on redox polymer/carbon nanotube modified electrodes: a review, Anal. Chim. Acta 881 (2015) 1–23.

[2] R. Li, Q. Tang, L. Yu, X. Yan, Z. Zhang, P. Yang, Counter electrodes from conducting polymer intercalated graphene for dye-sensitized solar cells, J. Power Sources 309 (2016) 231–237.

[3] A. Guerfi, J. Trottier, C. Gagnon, F. Barray, K. Zaghib, High rechargeable sodium metal-conducting polymer batteries, J. Power Sources 335 (2016) 131–137.

[4] M.E. Ghica, C.M.A. Brett, Poly(brilliant cresyl blue) modified glassy carbon electrodes: electrosynthesis, characterisation and application in biosensors, J. Electroanal. Chem. 629 (2009) 35–42.

[5] D. Benito, J.J. García-Jareño, J. Navarro-Laboulais, F. Vicente, Electrochemical behaviour of poly(neutral red) on an ITO electrode, J. Electroanal. Chem. 446 (1998) 47–55.

[6] M. Chen, J.Q. Xu, S.N. Ding, D. Shan, H.G. Xue, S. Cosnier, M. Holzinger, Poly(brilliant cresyl blue) electrogenerated on single-walled carbon nanotubes modified electrode and its application in mediated biosensing system, Sensor. Actuator. B Chem. 152 (2011) 14–20.

[7] D.W. Yang, H.H. Liu, Poly(brilliant cresyl blue)-carbon nanotube modified electrodes for determination of NADH and fabrication of ethanol dehydrogenase-based biosensor, Biosens. Bioelectron. 25 (2009) 733–738.

[8] K.C. Lin, J.Y. Huang, S.M. Chen, A low cost counter electrode using poly(-brilliant cresyl blue) and multi-walled carbon nanotubes for dye-sensitized solar cells, Int. J. Electrochem. Sci. 7 (2012) 12786–12795.

[9] M. Ding, Y. Zhou, X. Liang, H. Zou, Z. Wang, M. Wang, J. Ma, An electrochemical sensor based on graphene/poly(brilliant cresyl blue) nanocomposite for determination of epinephrine, J. Electroanal. Chem. 763 (2016) 25–31.

[10] P. De Los Santos Álvarez, M.J. Lobo-Castañón, A.J. Miranda-Ordieres, P. Tuñón-Blanco, Electrocatalytic oxidation of NADH by brilliant cresyl blue-DNA intercalation adduct, Electrochim. Acta 50 (2005) 1107–1112.

[11] M.E. Ghica, C.M.A. Brett, Poly(brilliant green) and poly(thionine) modified carbon nanotube coated carbon film electrodes for glucose and uric acid biosensors, Talanta 130 (2014) 198–206.

[12] P. Kubisa, Ionic liquids as solvents for polymerization processes - progress and challenges, Prog. Polym. Sci. 34 (2009) 1333–1347.

[13] B.D. Mather, N.M. Reinartz, M.B. Shiflett, Polymerization of vinyl fluoride in ionic liquid and ionic solutions, Polymer 82 (2016) 295–304.

[14] L.I.N. Tomé, V. Baião, W. da Silva, C.M.A. Brett, Deep eutectic solvents for the production and application of new materials, Appl. Mater. Today. 10 (2018) 30–50.

[15] J.D. Mota-Morales, R.J. Sánchez-Leija, A. Carranza, J.A. Pojman, F. del Monte, G. Luna-Bárcenas, Free-radical polymerizations of and in deep eutectic solvents: green synthesis of functional materials, Prog. Polym. Sci. 78 (2018) 139–153.

[16] A.P. Abbott, D. Boothby, G. Capper, D.L. Davies, R.K. Rasheed, Deep eutectic solvents formed between choline chloride and carboxylic acids: versatile alternatives to ionic liquids, J. Am. Chem. Soc. 126 (2004) 9142–9147.

[17] K. Ghandi, A review of ionic liquids, their limits and applications, Green Sustain. Chem. 4 (2014) 44–53.

[18] T.P. Thuy Pham, C.W. Cho, Y.S. Yun, Environmental fate and toxicity of ionic liquids: a review, Water Res. 44 (2010) 352–372.

[19] K. Mylvaganam, L.C. Zhang, Fabrication and application of polymer composites comprising carbon nanotubes, Recent Pat. Nanotechnol. 1 (2007) 59–65.

[20] M.E. Ghica, C.M.A. Brett, Simple and efficient epinephrine sensor based on carbon nanotube modified carbon film electrodes, Anal. Lett. 46 (2013) 1379–1393.

[21] R. Pauliukaite, M.E. Ghica, O. Fatibello-Filho, C.M.A. Brett, Comparative study of different cross-linking agents for the immobilization of functionalized carbon nanotubes within a chitosan film supported on a graphite-epoxy composite electrode, Anal. Chem. 81 (2009) 5364–5372.

[22] A.A. Balamurugan, S.M. Chen, Electrochemical preparation of composite of poly brilliant cresyl blue (PBCB)-poly 5-amino-2-napthalenesulfonic acid electrode and electrocatalytic application, J. Solid State Electrochem. 14 (2010) 35–41.

[23] L. Shen, X. Huang, Electrochemical polymerization of aniline in a protic ionic liquid with high proton activity, Synth. Met. 245 (2018) 18–23.

[24] N. Yi, M.R. Abidian, Conducting polymers and their biomedical applications, in: Biosynthetic Polym. Med. Appl., Woodhead Publishing, Cambridge, 2015.

[25] V. Pfaffen, P.I. Ortiz, S.I. Córdoba de Torresi, R.M. Torresi, On the pH dependence of electroactivity of poly(methylene blue) films, Electrochim. Acta 55 (2010) 1766–1771.

[26] A. Malinauskas, G. Niaura, S. Bloxham, T. Ruzgas, L. Gorton, Electropolymerization of preadsorbed layers of some azine redox dyes on graphite, J. Colloid Interface Sci. 230 (2000) 122–127.

[27] R. Pauliukaite, C.M.A. Brett, Poly(neutral red): electrosynthesis, characterization, and application as a redox mediator, Electroanalysis 20 (2008) 1275–1285.

[28] O. Hosu, M.M. Bârsan, C. Cristea, R. Săndulescu, C.M.A. Brett, Nanostructured electropolymerized poly(methylene blue) films from deep eutectic solvents. Optimization and characterization, Electrochim. Acta 232 (2017) 285–295.

[29] E. Laviron, General expression of the linear potential sweep voltammogram in the case of diffusionless electrochemical systems, J. Electroanal. Chem. 101 (1979) 19–28.

[30] E. Barsoukov, J.R. Macdonald, Impedance Spectroscopy: Theory, Experiment, and Applications, John Wiley & Sons, Inc., Hoboken, New Jersey, 2005.

[31] R. Pauliukaite, M.E. Ghica, O. Fatibello-Filho, C.M.A. Brett, Electrochemical impedance studies of chitosan-modified electrodes for application in electrochemical sensors and biosensors, Electrochim. Acta 55 (2010) 6239–6247.

[32] H. Yi, D. Zheng, C. Hu, S. Hu, Functionalized multiwalled carbon nanotubes through in situ electropolymerization of brilliant cresyl blue for determination of epinephrine, Electroanalysis 20 (2008) 1143–1146.

[33] H. Liu, G. Wang, J. Hu, D. Chen, W. Zhang, B. Fang, Electrocatalysis and determination of uracil on polythionine/multiwall carbon nanotubes modified electrode, J. Appl. Polym. Sci. 107 (2008) 3173–3178.

[34] Y. Xu, Y.-Z. Fang, Y. Wang, Y. Fang, Enhancement of electrochemical capacitance of carbon nanotubes by polythionine modification, Chin. J. Chem. 28 (2010) 417–421.

[35] A. Geto, C.M.A. Brett, Electrochemical synthesis, characterisation and comparative study of new conducting polymers from amino-substituted naphthalene sulfonic acids, J. Solid State Electrochem. 20 (2016), 2969-29-79.

[36] K.C. Lin, J.Y. Huang, S.M. Chen, Poly(brilliant cresyl blue) electrodeposited on multi-walled carbon nanotubes modified electrode and its application for persulfate determination, Int. J. Electrochem. Sci. 7 (2012) 9161–9173.

[37] S.A. Kumar, S.-F. Wang, Y.-T. Chang, Poly(BCB)/Au-nanoparticles hybrid film modified electrode: preparation, characterization and its application as a non-enzymatic sensor, Thin Solid Films 518 (2010) 5832–5838.

[38] C.M.A. Brett, A.M. Oliveira Brett, Electrochemistry. Principles, Methods and Applications, Oxford University Press, Oxford, 1993.

[39] M.M. Barsan, C.M.A. Brett, A new modified conducting carbon composite electrode as sensor for ascorbate and biosensor for glucose, Bioelectrochemistry 76 (2009) 135–140.

[40] H.F. Cui, K. Zhang, Y.F. Zhang, Y.L. Sun, J. Wang, W. De Zhang, J.H.T. Luong, Immobilization of glucose oxidase into a nanoporous TiO_2 film layered on metallophthalocyanine modified vertically-aligned carbon nanotubes for efficient direct electron transfer, Biosens. Bioelectron. 46 (2013) 113–118.

[41] V. Mani, B. Devadas, S.M. Chen, Direct electrochemistry of glucose oxidase at electrochemically reduced graphene oxide-multiwalled carbon nanotubes hybrid material modified electrode for glucose biosensor, Biosens. Bioelectron. 41 (2013) 309–315.

[42] Z. Luo, L. Yuwen, Y. Han, J. Tian, X. Zhu, L. Weng, L. Wang, Reduced graphene oxide/PAMAM-silver nanoparticles nanocomposite modified electrode for direct electrochemistry of glucose oxidase and glucose sensing, Biosens. Bioelectron. 36 (2012) 179–185.

[43] M. Cerrato-Alvarez, E. Bernalte, M.J. Bernalte-García, E. Pinilla-Gil, Fast and direct amperometric analysis of polyphenols in beers using tyrosinase-modified screen-printed gold nanoparticles biosensors, Talanta 193 (2019) 93–99.

[44] S. Tembe, S. Inamdar, S. Haram, M. Karve, S.F. D'Souza, Electrochemical biosensor for catechol using agarose-guar gum entrapped tyrosinase, J. Biotechnol. 128 (2007) 80–85.

[45] M. Sánchez-Paniagua López, B. López-Ruiz, Electrochemical biosensor based on ionic liquid polymeric microparticles. An analytical platform for catechol, Microchem. J. 138 (2018) 173–179.

[46] B. Pérez-López, A. Merkoçi, Magnetic nanoparticles modified with carbon nanotubes for electrocatalytic magnetoswitchable biosensing applications, Adv. Funct. Mater. 21 (2011) 255–260.